Journal of Theoretical and Applied Information Technology
15th November 2019. Vol.97. No 21

ISSN: 1992-8645 www.jatit.org E-ISSN: 1817-3195

A REVIEW OF DIGITAL BREAST TOMOSYNTHESIS HARDWARE TECHNIQUES

ABUAJELA ARHUMA GHUMEDH[1], S.MASHOHOR[2] , W.A.W ADNAN[3], ROZI MAHMUD[4]

[1]Department of Computer and Communication Systems, Faculty of Engineering, Universiti Putra Malaysia, 43400, Selangor, Malaysia
[2]Department of Computer and Communication Systems, Faculty of Engineering, Universiti Putra Malaysia, 43400, Selangor, Malaysia
[3]Department of Computer and Communication Systems, Faculty of Engineering, Universiti Putra Malaysia, 43400, Selangor, Malaysia
[4]Department of imaging, Faculty of Medicine and Health Science, Universiti Putra Malaysia, 43400, Selangor, Malaysia
[1]abouj1047@gmail.com, [2]Syamsiah@upm.edu.my, [3]wawa@upm.edu.my, [4]rozi@upm.edu.my

ABSTRACT

Digital Mammography (DM) technique is a well-rooted mode of imaging for early breast cancer detection and diagnosis. After the introduction of digital imaging in the field of radiology, several progressive methodologies have been developed, specifically tomographic imaging methodologies that are capable of capturing intricate details. The three dimensional (3D) Digital Breast Tomosynthesis (DBT) is one of such methodologies which has witnessed extensive penetration in clinics and possesses the capabilities to replace DM for the screening of breast cancer in the future. A lot of pre-acquisition processes of DBT influence its performance clinically. Therefore, this research focuses on the comprehensive review of the DBT system hardware design, the X-ray supply geometry optimization, radiation dose for breast glandular tissue, X-ray image scatter and breast compression minimization.

Keywords: *Digital Breast Tomosynthesis, Acquisition Geometry, Image Acquisition, Radiation Dose, X-Ray Scatter.*

1. INTRODUCTION

Standard mammography is a preferred mode of imaging as it is non-invasive, cost-efficient and time-efficient. It involves comparatively low, ionising radiation doses, but the Digital Mammography (DM) which has a two Dimensional (2D) attribute leads to a superposition of tissues. therefore, imposes two challenges: the decrease in the visibility of the lesion (impacting sensitivity), found in glandular tissue density positioned below and/or above a lesion, and the vertically-separated nature of two or more regular tissue structures, seems to be exactly the same as the projection of a lesion (decreasing specificity), both phenomena result in a sensitivity and specificity of 83.5%, and 90.9% respectively for DM screening [1]. However, for women with dense breasts, these values may be lower [2, 3, 4].

An introduction of digital procurement has enabled improvements in DM. One of the numerous issues that are mitigated by digital acquisition includes avoidance of the screen-films limited range of linear response. Then again, a 2D projection is obtained from a traditional mammography from its corresponding (3D) object, keeping the superposition of breast tissue problem unresolved. The utmost improvement in DM is probably its adjustability. This enables the advancement in imaging methodologies which eliminates some of the constraints of DM. To annul the information losses observed in the third dimension, there were two new imaging methodologies developed. They include; Computed Tomography (CT) image of the breast and dedicated DBT [5, 6, 7, 8, 9, 10, 11]. Although the dedicated breast CT has a lot of potentials, the DBT is presently the most growing technology in the clinical field. It has been approved for clinical use in the United States of America (USA) and across the world (refer to Table I). In DBT, a limited number of X-ray projections are acquired from a narrow angular range that enables pseudo tomographic imaging, and then these projections are combined to reconstruct a pseudo-3D image. The development of DBT has been discussed in-depth by the authors in [12, 13]. In 1997, the DBT imaging was initially proposed by Niklason et al. In the DBT imaging of the breast, the acquisition geometry is comparable to that utilized in DM, the only distinguishing factor being, the rotation of the x-ray tube about a plane, around the breast

ISSN: 1992-8645 www.jatit.org E-ISSN: 1817-3195

which is statically compressed and a sequence of images are realized with one at either side of the x-ray tube location (Figure. 2). The detector can be fixed or rotates during the acquisitions in order to preserve its top- most surface, which is normal to the x-ray tube [14, 15]. A reconstruction algorithm is implemented to process the series of projections acquired. The algorithm uses various locations to project the same tissues so that their vertical position can be calculated and thereby the 3D distribution of the tissues can be estimated. As a result of the restricted angle of projection acquisitions, the DBT is distinguished using the anisotropic spatial resolution, with considerably low resolution in the perpendicular direction, and the planes which are parallel in direction to the detector, exhibit very large spatial resolution. Further, the low anisotropic spatial resolution within the depth's path is considered as adequate in the minimization of the problem of tissue superposition considerably, thereby reducing its effect on sensitivity and specificity.

Therefore, this paper will review the image acquisition methods involved in DBT imaging.

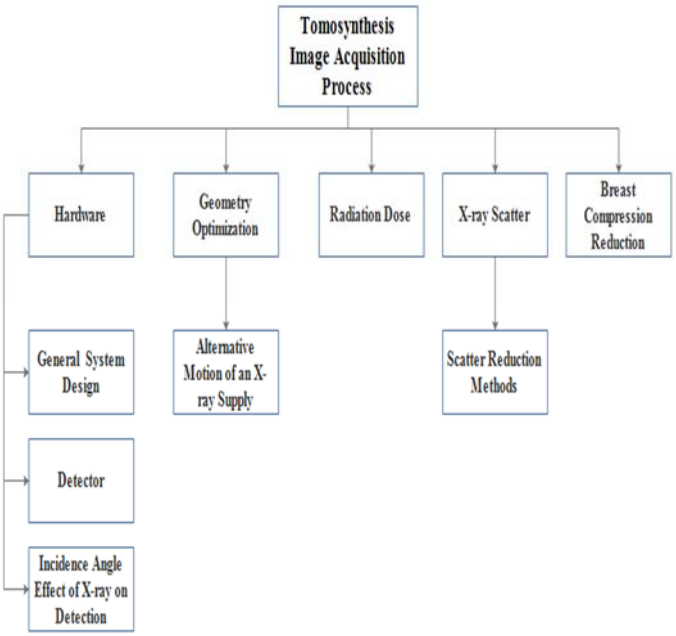

Figure 1: Block Diagram For DBT Pre-Acquisition Processes

2. HARDWARE

2.1 General System Design

At present, the majority of the DBT systems constitute of identical elementary modules as digital mammography systems, which include the arm that holds the x-ray tube, a breast support and compression plate and a direct or indirect complete field digital detector. The transformation of a DM system into a DBT system is achieved through the addition of a specific basic hardware, which is the x-ray tube that has the ability to rotate around a point on or near to the detector, where the detector has a comparatively high-speed readout. More extra modifications have certainly been applied by the manufacturers to ensure that the DBT system acquisition is optimized more against the DM acquisition, which for instance involves various pixel binning and x-ray spectrum filtration [26, 27]. In recent studies, the researchers have substituted the x-ray tube, as well as the commercial DBT system's gantry (Hologic Selenia Dimensions, Incorporated, Bedford) with a nanotube array made of carbon that spans 370 mm leading to an angular coverage of 30° and has 31 x-ray sources. A developed Modulation Transfer Function (MTF) was yielded by the stationary x-ray source compared to a typical rotating x-ray tube. An improvement in the sharpness of phantom microcalcification images was also observed for the stationary x-ray source. Some of the challenges that are still unresolved, and needed to improve the overall scan time include exposure time and x-ray tube current, and detector readout rate [28, 29, 30]. The latest version of the photon counting detector is made up of a mechanism of energy resolution, which enables the acquisition of two images simultaneously [32]. In spite of this, the tomosynthesis system cannot acquire mammographic images because of the system's acquisition geometry. Some research had been conducted on an identical slot scanning photon and its development had been suspended [33]. Table1 provides a summary of the attributes of the various tomosynthesis systems that are presently under pre-clinical or clinical use.

2.2 Detectors

In order to optimize the detectors for DBT imaging, extensive work has been carried out. Besides the requisites for DM, the detectors for DBT are required to attain added capabilities. A few of the desired capabilities include: (i) minimal lag and ghosting, which leads to the introduction of image artefacts [34, 35], (ii) faster reading time to limit the total acquisition time of all projections to a minimum, and (iii) low minimization in the Detective Quantum Efficiency (DQE), at little exposures. As anticipated, there was an improvement in the binned mode results, with respect to the Signal-to-Noise Ratio (SNR),

ISSN: 1992-8645 www.jatit.org E-ISSN: 1817-3195

on the other hand, it possessed a retribution in the MTF binning path that was aligned to the x-ray's supply movement. The binned mode further diminished the fall in DQE with reducing exposure, which was however comparatively low for the complete resolution mode. In contrast, there was a higher lag, with a binned detector, while for both modes, and the ghosting was insignificant. At the minimum exposure levels, it was further observed that the DQE compared to DBT reduction of about 20% only as against the high levels of exposure.

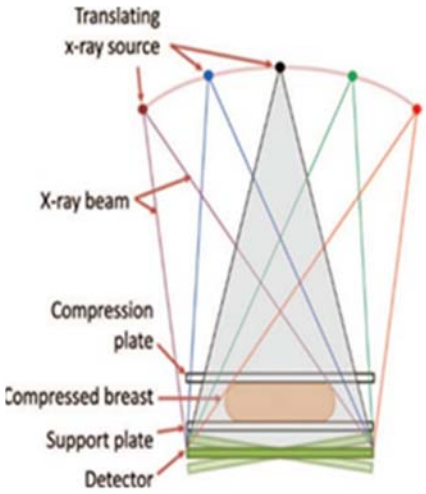

Figure 2: Schematic Of A DBT Acquisition [31]

2.3 Incidence angle effect of X-ray on Detection

Due to the presence of the stationary detector in DBT systems, the x-ray's angle of incidence onto the detector could be considerably enormous. The outcomes of this enormous angle of incidence over the MTF have been studied analytically, as well as the Monte Carlo (MC) simulations for the direct Selenium (Se) detectors, the scintillator-based indirect detectors, and the empirical study of the Point Spread Function (PSF) [37, 38, 39, 40, 41]. Badano et al. first studied the impact over the PSF in the presence of indirect detectors, using MC techniques, where the results of the study revealed the anisotropy presented by the abnormal incidence, and its fluctuation all through the surface of the detector, as a result of the variable angle of incidence [42, 43].

In a subsequent study on the same work, a systematic model was devised for the detectors, and the empirical study of the Point Spread Function (PSF) [37, 38, 39, 40, 41]. Badano et al. first studied the impact over the PSF in the presence of indirect detectors, using MC techniques, where the results of the study revealed the anisotropy presented by the abnormal incidence, and its fluctuation all through the surface of the detector, as a result of the variable angle of incidence [42, 43].

ISSN: 1992-8645 www.jatit.org E-ISSN: 1817-3195

DBT systems		FUJIFILE Amulet Innoyality [16, 17]	IMS Giotto TOMO [18, 19]	Planmed Nuance Excel DBT [20, 21]	Hologic Selenia Dimension [22]	Philips Micro- Dose [23]	Siemens Mammomat Inspiration [22, 24, 25]	GE Essential [22]
X-ray tube	Filtration	0.7 mm Aluminium (Al)	0.05mm Rhodium (Rh) or 0.05mm Silver (Ag)	0.075mm Silver (Ag) or 0.06mm Rhodium (Rh)	0.7mm Aluminium (Al)	0.5mm Aluminium (Al)	0.05mm Rhodium (Rh)	0.03mm Molybdenum (Mo) or 0.025mm Rhodium (Rh)
	Motion	Continuous	Step and shoot	Continuous	Continuous	Continuous	Continuous	Step and shoot
Detector	Type	Full field- direct amorphous selenium (a-se	Full field-direct amorphous (a-se)	Full field-direct amorphous selenium (a-se)	Full field-direct amorphous (a-se)	Line slit Scan- spectral photon counting silicon (Si)	Full field- direct amorphous selenium (a-se)	Full field-indirect
	Size (cm)	24x30	24x30	24x30	24x29	21 line detectors, each 24cm long	24x30	24x30
	Pixel size (1m)	150 (ST binned 2x1)	85	85	70 (binned 2x2)	50 (perpendicul ar to motion)	85	10
	Motion	Static	Static	Rotating during exposure b	Rotating	Continuous slit scan	Static	Static
Acquisition	Grid	No	No	No	No	No	No	Yes
	Angular range (deg)	40 (HR) 15 (ST)	40	30	15c	11	50	25
	Number of Projection	15	13c	15	15	21	25	9
	Scan time (s)	9 (HR) 4 (ST)	12	20	3.7	3-10	25	7
	Source to detector distance (cm)	65	68	65	70	66	66.5	66
	Detector to center of rotation distance (cm)	4	2	4.37	0	-40	4.7	4
Reconstruction	Method	Filtered Back Projection (FBP)	Iterative with total variation regularisation	Iterative	Filtered Back Projection (FBP	Iterative	Filtered Back Projection (FBP)	Iterative

Table 1: Specification of clinical of Digital Breast Tomosynthesis systems

ISSN: 1992-8645 www.jatit.org E-ISSN: 1817-3195

and its fluctuation all through the surface of the detector, as a result of the variable angle of incidence [42, 43]. In a subsequent study on the same work, a systematic model was devised for the calculation of the PSF feasible for the indirect detectors under varying environments, without executing the CPU-intensive MC simulations by Freed et al. The same model was further developed to determine the PSF for direct detectors [44].

In this study, these analytical models had been used to understand the dependence of these metrics on the angle of incidence of the x-rays and on the design of the detectors.

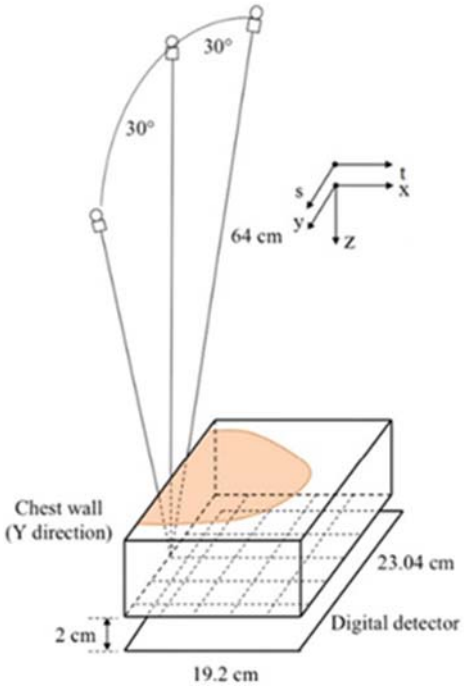

Figure 3: Digital Detector In DBT Imaging [36]

It was observed that the backside-illuminated detectors were limitedly responsive and susceptible to the incidence angle than the front-illuminated detectors, and hence, for DBT imaging, the backside-illuminated detectors would be more appropriate, because it was less sensitive.

3. GEOMETRY OPTIMIZATION

The acquisition of a DBT image, like most other medical imaging modalities, includes a number of parameter selections. The highly researched parameter acquisitions in DBT are the ones which play a significant role in defining the acquisition geometry which are the projections covered the total angular range, the distribution of the projections, and the number of projections. Table I shows the enormous differences in the values of the geometrical parameters that are used in the latest tomosynthesis systems. The complexity involved in optimizing these parameters are indicated by the values presented in the table. Theoretically, it would be presumed that by augmenting the projection number and the angular range, the utmost quality of image could be attained. In the end, for different angles of projection, the probability of applying varying tube current exposure time and/or allowing a random distribution of the angles of projection intensifies the complexity of the optimization problem over the range of angles. This might also improve the image quality, particularly for specific clinical procedures (for example, soft tissue lesion or microcalcification detection) [45, 46]. Maidment et al. conducted a wire-based DBT imaging simulation and visualized a rabbit image that possessed a photon-counting DBT system [33]. The objective of this experiment was to investigate the geometrical parameter optimal values that are related to the imaging of the DBT. The wire simulations were carried out devoid of any additional noise. It was observed that increasing the projection number and angular range led to a protocol with an optimal acquisition. After the analysis of the projection number's impact involved with the DBT set for a second time via the use of clinical images, increasing the number of projections to a maximum, resulted in improved image quality [25]. In one more study conducted by Ren et al. with the help of a homogeneous phantom. It was observed that augmenting the projection number for a range of angles and a certain overall dose would result in a minute improvement in the CNR's vertical profile. Whereas there was a degradation in the in plane image quality due to the increased number of projections [47].Four various acquisition protocols (the use of 2-2 pixels binning was included in a fifth variation) were also compared in a simulation-based study. By employing a homogeneous background, a monochromatic x-ray beam and three distinctive reconstruction techniques conducted by Zhou et al. In this study, the authors made use of a Signal-to-Noise Ratio (SNR) for assessing in-plane image quality. While in contrast, for vertical resolution in DBT imaging, the researchers utilized a typical metric, referred to as an Artefact Spread Function (ASF) [48]. Which is defined in the equation below.

$$ASF(Z) = \frac{I_S(Z) - I_{BG}(Z)}{I_S(Z_0) - I_{BG}(Z_0)} \quad (1)$$

ISSN: 1992-8645 www.jatit.org E-ISSN: 1817-3195

Where I_s refers to the signal mean value of the pixel, I_{BG} refers to the background mean value of the pixel, Z is the current location and Z_0 is the in-focus plane's location. With these metrics, the projections number and maximized range of angles led to an optimized image quality, established by Zhou et al. Ghetti and Sechopoulos further validated

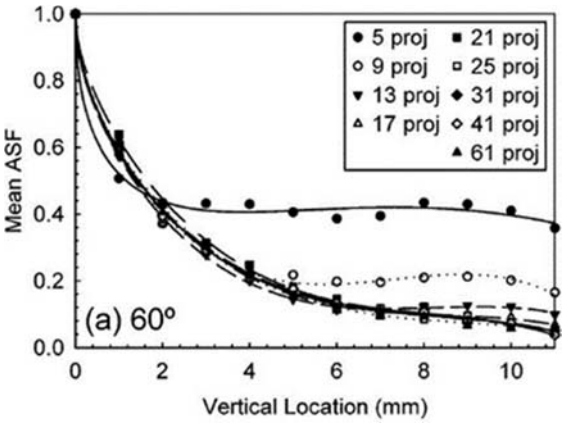

Figure 4: ASF From Simulated DBT Images Acquired With Varying Projection Number And A 600 Range Of Angles. [49]

the same observation and additionally found that, by augmenting the projection number for each range of angles beyond a limit to reduce the artefacts of the off-focus plane, did not yield improvement or the desired result in the vertical resolution infinitely (Figure. 4) [50]. In this study, the author had suggested the "quality factor" metric to analyze these relationships. The "quality factor" is a mixture of the vertical resolution and the in-plane image quality, which functions as a metric to correlate the DBT's image quality and is expressed as:

$$QF = \frac{CNR}{ASF_W} \qquad (2)$$

Here, CNR refers to a measure of the quality of an in-plane image. ASF_w refers to the ASF's width. For example, the z location is the point where the ASF (z) in equation (1) reaches an amount of 0.2. As shown in Figure 4, the angles for the number of projection necessary for attaining a "threshold", above which there is no more improvement, is considerably low in the vertical resolution for a certain range of angles. With a common QF metric, Tucker et al conducted a study using x-ray sources with a stationary carbon nanotube and made an identical conclusion on the effect of the range of angles, and the DBT's projection number [28].

3.1 Alternative Motion of an X-ray Supply

As depicted in Fig. 2, in the designs for standard DBT, the X-ray supply progresses in a plane about an arc, over the breast that undergoes imaging. Additional designs for DBT have been suggested. Stevens et al introduced a Circular DBT, in which the detector and the X-ray supply moved in a circular plane that was aligned to one another [51]. On the other hand, Zeng et al. recommended combining the DBT acquisition with the acquisition of a CT scan to achieve an enhanced reconstruction quality, where a high rate of resolution DBT image obtained using a standard arc motion, was combined with a low rate of resolution CT image, obtained through an arc-and-line motion [52]. Xia et al. suggested relocating the X-ray supply in both arcs, which were normal to one another, so that a spherical surface part beyond the imaged object could be encircled [53]. Zhang and Yu also suggested this geometry, where the source rotation was combined with the rotation of the detector, and a different way was presented to encompass the spherical surface, which was a succession of curved zigzag lines as shown in Figure. 5 [54]. With the use of the two architectures in tandem, the advantage was that the frequency domain could be sampled more comprehensively, leading to an enhanced image quality. However, there were potential geometrical issues with the remaining parts of the patient's body that needed to be examined for these geometries to be effective clinically.

4. RADIATION DOSE

The radiation dose accumulated in the breast's glandular tissue is a risk of cancer improvement during breast imaging. Hence, the Mean Glandular Dose (MGD) was recommended as

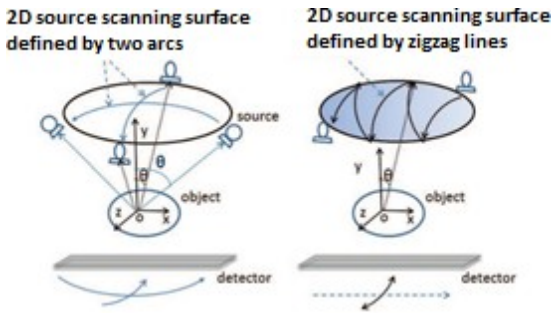

Figure 5: Alternative X-Ray Source Motions For The Acquisition Of DBT Projections [54]

a cadence for the breast scan's dosage. Conventionally, MGD was measured using the Monte Carlo approach which simulated the acquisition process that was implemented to quantify the energy accumulated by the breast in the glandular area. The breast

ISSN: 1992-8645 www.jatit.org E-ISSN: 1817-3195

representation was generally done very much like the adipose- glandular tissue composition with a skin layer enclosure. In general, the air karma in front of the breast surface acts like a normalising factor for the MGD, which results in a Normalised mean Glandular Dose (D_gN), expressed as the Mean Glandular Dose (M_gD) per unit mGy air kerma, with a unit of mGy. To clarify the assessment of the overall MGD in DBT from an entire acquisition, the Relative Glandular Dose (RGD) metric was introduced, and it is expressed as in the equation below [55].

$$RGD(\alpha) = \frac{D_gN(\alpha)}{D_gN_0} \quad (3)$$

Where (D_gN_0) (D_g) N(α) refer to the normalised glandular dose values for the angles of projection 0° and α, correspondingly. Hence, under the same environments, α is comparable to the (D_gN) for a DM acquisition. With the help of the RGD, the overall (D_g) N for an entire DBT acquisition can be calculated as follows:

$$D_gN = D_gN_0.\sum_\alpha RGD(\alpha) = D_gN_0 \,.N_\alpha.\mu_{RGD} \quad (4)$$

Where $N(\alpha)$ refers to the number of projections attained, and (μ_{RGD}) refers to the RGD mean included in the DBT acquisition, for the angles of projection. If a DBT acquisition leads to a μ_{RGD} of unity, then D_gN can be computed by multiplying the applicable D_gN_0 by the projection number in the acquisition. For some specific acquisition environments, such as small overall range of angles, and for a few varying breast sizes and thicknesses, the estimated (μ_{RGD}) had been found to be very close to unity [56].

5. X-RAY SCATTER

In an X-ray image, the addition, as well as the identification of the X-ray image scatter signal, in the captured images lead to a range of effects that include loss of accuracy, dependency on modality, and loss of contrast. In a digital mammogram, the scattering of X-ray signals are mitigated by anti-scatter grids utilization that is positioned between a detector, and the breast, that satisfactorily consume scattered X-rays, as well as transfer non-scattered X-rays. However, anti-scatter frameworks are certainly less impeccable solutions as these include a consequential increased dose of X-rays to the breast, in order to attain a non-grid signal strength about the detector [43, 57, 58]. In DBT, there are two important reasons why the scatter of an X-ray is more important than DM: (i) the changeable comparative X-ray supply's location with a static detector will cause an acute saturation of the primary X-rays, by the grid at non-zero angles of projection, (ii) the already low exposure available for every projection would be lowered further due to the inclusion of a grid. In a study conducted on scatter characterisation, the Monte Carlo technique was used by Sechopoulos et al. to compute the Scatter-to-Primary Ratio (SPR), and scatter PSF for different breast definitions, and imaging conditions [59, 60]. In this study, the authors observed that with an increase in the projection angle, the pieces of the PSF scatter across the opposite side to the X-ray tube position expanded, while the tails at the identical side of the X-ray tube position tapered. Moreover, as observed in earlier DM results, [58, 61] there was no substantial variance in the PSF scatter with the spectrum of the X-ray, and only a small variance occurred alongside the Breast Glandular Fraction (BGF). The study of the SPR led to polynomial-fit equations that were used to find the SPR at the breast's projection mass centre. The SPR is a glandular fraction of breast thickness and the DBT projection angle. The advantage of this technique as stated by the authors was that, the impact the X- ray scatter had on DBT image quality was clear and substantial, both in mammography and DBT. However, its effect on clinical performance is yet to be investigated [62, 63, 64].

5.1 Scatter Reduction Methods

Correction methods and X-ray scatter reduction can be deemed as advantageous for improving image quality in DBT. Liu et al. suggested one such scatter reduction method that was based on a software method and required no extra hardware [65]. In the recommended approach, after the reconstruction of the DBT breast image, the available voxels in the image of the breast that were reconstructed, were linked to a restricted amount of various mixtures of glandular tissues and adipose with calcium. The 3D image was subsequently categorized and put in an MC simulation system in order to analyze and project the distribution of the scatter signal in the projections. However, a rise in noise level was observed as anticipated, through the decrease in the overall signal. X-ray scatter correction algorithms based on low-frequency scatter signal subtraction from the acquired projections without reducing the scatter quantum noise. it is characterized by increasing noise through a decrease of the overall signal [63, 65]. Feng and Sechopoulos suggested leveraging the scatter distribution's known insensitivity to breast composition, and size to execute a scatter correction based on a model, in order to reduce the computation time required for the patient-peculiar MC simulations [66].

6. Breast Compression Minimization

It has been suggested that DBT imaging could be

ISSN: 1992-8645 www.jatit.org E-ISSN: 1817-3195

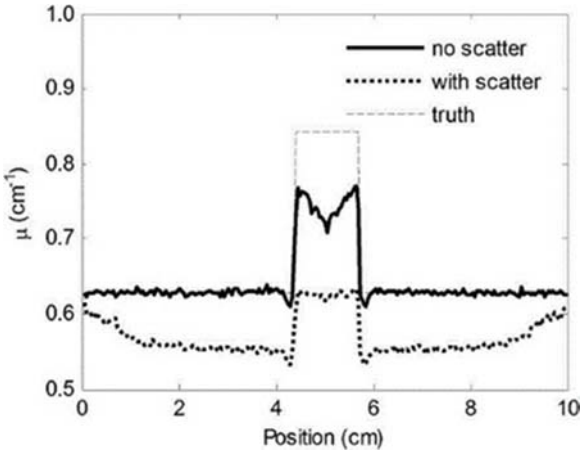

Figure 6: Horizontal Sketch Via The Centre Of A Lesion In A DBT Reconstructed Slice Indicating A Decrease In The Values Of The Voxels, As Well As A Contrast Owing To An X-Ray Scatter Existence [62]

executed with a considerable minimization in the mechanical compression of the breast, employed in the course of acquisition when matched to DM. This can inherently minimize the issue of tissue superposition faced in the imaging of planes. The authors' employed lesion conspicuity for calcifications and masses and then found that there was no significant contrast in the minimized compression, even on changing the exposure parameters, in order to continue with a fixed dose for the breasts. A clinical study was done by Fornvik et al. By acquiring DBT images of patients with partly the force employed in full compression and with full compression, via identical acquisition technique for both [67, 68]. In breast imaging, even though the key reason for breast compression is the minimization of tissue superposition, there are other reasons as well. Other necessary considerations for breast compression include motion artefacts and breast dose, a decrease in the scatter signal of an x-ray and a rise in the number of breast tissues in the terrain of view. Therefore, before clinically carrying out DBT with reduced compression, it should be confirmed if a reduction in compression force would adversely impact these other factors [69].

6. DISCUSSION:

This paper discusses characteristic of all digital breast tomosynthesis systems that are variable in clinical. It is understandable that parameters of digital breast tomosynthesis imaging that are used in post-processing. Also, the different methods of reconstruction were used for each system of tomosynthesis. Although the use of objective metrics such as CNR and ASF yield useful comparative information on image quality, they do not provide any absolute relation to diagnostic quality, for which perception based image quality models are needed. Many research have been performed on lots of the acquisition parameters and other physical aspects of DBT image acquisition, such as radiation dose and x-ray scatter. In many aspects, this has resulted a good understanding of the issues, with several different research approaches often arriving at similar conclusions.

7.1. Radiation dose

Tomosynthesis is a new digital mammography tool, with safe radiation doses within the allowed parameters, that is changing breast cancer diagnosis thanks to its better performance (improved sensitivity and specificity) in comparison with traditional 2D mammography. Radiation dosage is a major concern for the International Commission on Radiological Protection due to potential risks of ionizing radiation in unauthorized doses. Tomosynthesis is considered a safe procedure as radiation doses it requires are within parameters established by the Mammography Quality Standard. Since its approval for clinical use in 2013, multiple studies have demonstrated that use of synthesized mammography can decrease radiation dose by nearly half, while maintaining the performance benefits of DBT over FFDM. Although tomosynthesis lower resolution than FFDM, with 2Ds, cancer detection is preserved and the risks of missing a low-density finding is outweighed by this benefit as well as the decreased dose. Differences in the appearance of the 2Ds image exist and this may require an adjustment period. Future research avenues remain to optimize the usage of 2Ds.

7.2. X-ray scatter

The imaging performance of tomosynthesis is challenged by some physical factors, including detector efficiency, geometry alignment, and x-ray scatter. Several investigators have studied scatter properties in mammographic applications with experimental and analytical methods. Tomosynthesis is now becoming a new clinical standard, but there are currently no methods of alleviating the negative effects of scattered radiation on DBT image quality for a vast majority of clinical DBT systems. Tomosynthesis reconstructed images fall short of truth even in the absence of scatter. This is due to limitations in the reconstruction algorithm and the incomplete sampling geometry of tomosynthesis. The error in the reconstructions is further increased by the apparent signal increase due to the presence of scatter. The detection and inclusion of an x-ray scatter signal in images obtained in x-ray imaging obtained in wastage of contrast, amidst other effects such as wastage

ISSN: 1992-8645 www.jatit.org E-ISSN: 1817-3195

of accuracy, depending on the method. In mammography, the x-ray scatter was treated by the use of anti-scattering networks between the breast and the detector, which preferentially absorbed scattered x-ray absorption and the transfer of primary (non-scattered) x-rays. Therefore, anti-scattering networks are not ideal and include a penalty for increasing the dose to the breast to achieve the same signal at the detector.

Recently, researchers are trying to perform a better evaluation of the clinical impact of the algorithm on detection and diagnosis. One of the main disadvantages of most DBT systems is large scattered radiation fraction observed at the image receptor. For system modelling and optimization or scatter correction or removal, a good understanding of the scatter signal for each of the DBT projections is required.

To increase image quality, an optimal number of projections was achieved at a relatively low number. Other aspects a correction or reduction of the x-ray scatter signal in DBT projection, still necessitate further research before application in clinical DBT imaging. The software-based scatter correction algorithm on DBT imaging produced measurable improvement in the image quality of the scatters correction reconstructions. The application of methods to the reconstruction of images also improve the image quality, including those actionable findings in a clinical setting.

Current DBT systems, lack x-ray scatter reduction measures, be it in software or hardware. This leads to the inclusion of the entirety of the x-ray scatter signal in the tomosynthesis projections, resulting in reconstruction artifacts and reduced contrast. According to previously developed a software-based x-ray scatter correction algorithm that when the acquired tomosynthesis projections is applied before reconstruction, it shown potential in improving image quality.

Finally, the improved accuracy and overall efficiency that DBT can provide will enhance radiologists' performance and improve the patient experience. Future progressive improvements in DBT technology will likely decrease radiation exposure. In practice, women who require extra mammographic views (e.g., technical repeats, implants, or tiled large breasts) were originally not offered in DBT until we obtained the ability to perform synthesized mammography. It may help to clarify the issue over whether the adoption of new technical developments is able to improve the effective screening for breast cancer in a population-based context.

8. CONCLUSION

Lot of works on the factors of acquisition have been done and more visible facets of image acquisition in DBT that includes X-ray scattering and radiation dose. As a result, the aforementioned has brought about a great knowledge of the concerns, with many various investigated methodologies leading to comparable outcomes. This is seen in the maximum number of projections achieved and the improved image quality obtained from the use of a large angular range. Further works are needed to be done in the modification of X-ray scatter signals in DBT projections before it is applied in the clinical domain.

9. ACKNOWLEDGMETt:

I would like to thank Universiti Putra Malaysia (UPM), for providing technical and financial support during this title research under grant number 9665600 and Computer Aided Detection of Breast Cancer using Region Growing in automated 3D Breast Ultrasound.

REFERENCES

[1] B. C. S. Consortium, "Performance measures for 1,838,372 screening mammography examinations from 2004 to 2008 by age—based on BCSC data through 2009," ed, 2015.

[1] K. Kerlikowske, M. Grady, M. Barclay, and V. Ernster, "and Family His- tory on the Sensitivity of First Screening Mammography," Jama, vol. 276, 1996.

[2] P. A. Carney, D. L. Miglioretti, B. C. Yankaskas, K. Kerlikowske, R. Rosenberg, C. M. Rutter, et al., "Individual and combined effects of age, breast density, and hormone replacement therapy use on the accuracy of screening mammography," Annals of internal medicine, vol. 138, pp. 168- 175, 2003.

[3] C. M. Kuzmiak, E. B. Cole, D. Zeng, L. A. Tuttle, D. Steed, and E. D. Pisano, "Dedicated three-dimensional breast computed tomography: lesion characteristic perception by radiologists," Journal of clinical imaging science, vol. 6, 2016.

[4] J. M. Boone, T. R. Nelson, K. K. Lindfors, and J. A. Seibert,"Dedicated breast CT: radiation dose and image quality evaluation," Radiology, vol. 221, pp. 657-667, 2001.

[5] R. Ning, D. L. Conover, B. Chen, L. Schiffhauer, J. Cullinan, Y. Ning, et al., "Flat-panel-detector-based cone-beam volume CT breast imaging: Phantom and specimen study," in Medical Imaging 2002: Physics of Medical Imaging, 2002, pp. 218-228.

ISSN: 1992-8645 www.jatit.org E-ISSN: 1817-3195

[6] B. Chen and R. Ning, ”Cone-beam volume CT breast imaging: Feasibility study,” Medical physics, vol. 29, pp. 755-770, 2002.

[7] R. L. McKinley, M. P. Tornai, E. Samei, and M. L. Bradshaw, ”Initial study of quasi-monochromatic x-ray beam performance for x-ray computed mam- motomography,” IEEE transactions on nuclear science, vol. 52, pp. 1243-1250, 2005.

[8] R. L. McKinley, M. P. Tornai, C. Brzymialkiewicz, P. Madhav, E. Samei, and J. E. Bowsher, ”Analysis of a novel offset cone-beam computed mam- motomography system geometry for accomodating various breast sizes,” Physica Medica: European Journal of Medical Physics, vol. 21, pp. 48-55, 2006.

[9] K. K. Lindfors, J. M. Boone, T. R. Nelson, K. Yang, A. L. Kwan, and D.
F. Miller,”Dedicated breast CT: initial clinical experience,” Radiology, vol. 246, pp. 725-733, 2008.

[10] W. A. Kalender, M. Beister, J. M. Boone, D. Kolditz, S. V. Vollmar, and
M. C. Weigel, ”High-resolution spiral CT of the breast at very low dose: concept and feasibility considerations,” European radiology, vol. 22, pp. 1- 8, 2012.

[11] J. T. Dobbins III and D. J. Godfrey, ”Digital x-ray tomosynthesis: current state of the art and clinical potential,” Physics in medicine & biology, vol. 48, p. R65, 2003.

[12] J. T. Dobbins, ”Tomosynthesis imaging: at a translational crossroads,” Medical physics, vol. 36, pp. 1956-1967, 2009.

[13] B. Ren, C. Ruth, J. Stein, A. Smith, I. Shaw, and Z. Jing, ”Design and performance of the prototype full field breast tomosynthesis system with selenium based flat panel detector,” in Medical Imaging 2005: Physics of Medical Imaging, 2005, pp. 550-562.

[14] J. W. Eberhard, P. Staudinger, J. Smolenski, J. Ding, A. Schmitz, J. Mc- Coy, et al., ”High-speed large angle mammography tomosynthesis system,” in Medical Imaging 2006: Physics of Medical Imaging, 2006, p. 61420C.

[15] A. Maldera, P. De Marco, P. Colombo, D. Origgi, and A. Torresin, ”Dig- ital breast tomosynthesis: Dose and image quality assessment,” Physica Medica: European Journal of Medical Physics, vol. 33, pp. 56-67, 2017.

[16] A. Rodr´ıguez-Ruiz, M. Castillo, J. Garayoa, and M. Chevalier, ”Evalua- tion of the technical performance of three different commercial digital breast tomosynthesis systems in the clinical environment,” Physica Medica: European Journal of Medical Physics, vol. 32, pp. 767-777, 2016.

[17] S. Vecchio, A. Albanese, P. Vignoli, and A. Taibi, ”A novel approach to digital breast tomosynthesis for simultaneous acquisition of 2D and 3D images,” European radiology, vol. 21, pp. 1207-1213, 2011.

[18] R. Girometti, C. Zuiani, A. Taibi, S. Vecchio, R. Fazzin, and M. Baz- zocchi, ”Diagnostic yield of digital breast tomosynthesis (DBT) vs digital mammography (DM) in assessing breast cancer: A study on surgical specimens,” in European Congress of Radiology, Vienna, Austria, 2012.

[19] M. Varjonen, M. Pamilo, P. Hokka, R. Hokkanen, and P. Stro¨mmer, ”Breast positioning system for full field digital mammography and digital breast tomosynthesis system,” in Medical Imaging 2007: Physics of Medi- cal Imaging, 2007, p. 651036.

[20] R. Van Engen, R. Bouwman, D. Dance, P. Heid, B. Lazzari, N. Marshall, et al., ”Protocol for the quality control of the physical and technical aspects of digital breast tomosynthesis system,” EUREF, European Guidelines for Quality Assurance in Breast Cancer Screening and Diagnosis, 2013.

[21] J. A. Baker and J. Y. Lo, ”Breast tomosynthesis: state-of-the-art and re- view of the literature,” Academic radiology, vol. 18, pp. 1298-1310, 2011.

[22] I. Sechopoulos, J. M. Sabol, J. Berglund, W. E. Bolch, L. Brateman, E. Christodoulou, et al., ”Radiation dosimetry in digital breast tomosynthesis: Report of AAPM Tomosynthesis Subcommittee Task Group 223,” Medical physics, vol. 41, 2014.

[23] S. Young, S. Park, S. K. Anderson, A. Badano, K. J. Myers, and P. Ba- kic, ”Estimating breast tomosynthesis performance in detection tasks with variable-background phantoms,” in Medical Imaging 2009: Physics of Med- ical Imaging, 2009, p. 72580O.

[24] E. Shaheen, C. Van Ongeval, F. Zanca, L. Cockmartin, N. Marshall, J. Jacobs, et al., ”The simulation of 3D microcalcification clusters in 2D digi- tal mammography and breast tomosynthesis,” Medical physics, vol. 38, pp. 6659-6671, 2011.

[25] B. Ren, C. Ruth, T. Wu, Y. Zhang, A. Smith, L. Niklason, et al., ”A new generation FFDM/tomosynthesis fusion system with selenium detector,” in Medical Imaging 2010: Physics of Medical Imaging, 2010, p. 76220B.

ISSN: 1992-8645 www.jatit.org E-ISSN: 1817-3195

[26] L. Cockmartin, N. W. Marshall, G. Zhang, K. Lemmens, E. Shaheen,
C. Van Ongeval, et al., ”Design and application of a structured phantom for detection performance comparison between breast tomosynthesis and digital mammography,” Physics in Medicine & Biology, vol. 62, p. 758, 2017.

[27] X. Qian, A. Tucker, E. Gidcumb, J. Shan, G. Yang, X. Calderon-Colon, et al., ”High resolution stationary digital breast tomosynthesis using dis- tributed carbon nanotube x-ray source array,” Medical physics, vol. 39, pp. 2090-2099, 2012.

[28] J. Heggie, P. Barnes, L. Cartwright, J. Diffey, J. Tse, J. Herley, et al., ”Position paper: recommendations for a digital mammography quality as- surance program V4. 0,” Australasian physical & engineering sciences in medicine, vol. 40, pp. 491-543, 2017.

[29] C. Lee and J. Baek, ”A sphere phantom approach to measure directional modulation transfer functions for tomosynthesis imaging systems,” IEEE transactions on medical imaging, vol. 35, pp. 871-881, 2016.

[30] L. T. Niklason, B. T. Christian, L. E. Niklason, D. B. Kopans, D. E. Castleberry, B. Opsahl-Ong, et al., ”Digital tomosynthesis in breast imag- ing,” Radiology, vol. 205, pp. 399-406, 1997.

[31] F. F. Schmitzberger, E. M. Fallenberg, R. Lawaczeck, M. Hemmendorff,
E. Moa, M. Danielsson, et al., ”Development of low-dose photon-counting contrast-enhanced tomosynthesis with spectral imaging,” Radiology, vol. 259, pp. 558-564, 2011.

[32] A. D. Maidment, C. Ullberg, K. Lindman, L. Adelo¨w, J. Egerstro¨m, M. Eklund, et al., ”Evaluation of a photon-counting breast tomosynthesis imag- ing system,” in Medical Imaging 2006: Physics of Medical Imaging, 2006, p. 61420B.

[33] J. G. Mainprize, X. Wang, and M. J. Yaffe, ”The effect of lag on image quality for a digital breast tomosynthesis system,” in Medical Imaging 2009: Physics of Medical Imaging, 2009, p. 72580R.

[34] J. Zheng, J. A. Fessler, and H.-P. Chan, ”Detector Blur and Correlated Noise Modeling for Digital Breast Tomosynthesis Reconstruction,” IEEE transactions on medical imaging, vol. 37, pp. 116-127, 2018.

[35] J. Zheng, J. A. Fessler, and H.-P. Chan, ”Detector Blur and Correlated Noise Modeling for Digital Breast Tomosynthesis Reconstruction,” IEEE transactions on medical imaging, 2017.

[36] B. Zhao and W. Zhao, ”Imaging performance of an amorphous selenium digital mammography detector in a breast tomosynthesis system,” Medical physics, vol. 35, pp. 1978-1987, 2008.

[37] J. G. Mainprize, A. K. Bloomquist, M. P. Kempston, and M. J. Yaffe, ”Resolution at oblique incidence angles of a flat panel imager for breast tomosynthesis,” Medical physics, vol. 33, pp. 3159-3164, 2006.

[38] M. Freed, S. Park, and A. Badano, ”A fast, angle-dependent, analytical model of CsI detector response for optimization of 3D x-ray breast imaging systems,” Medical physics, vol. 37, pp. 2593-2605, 2010.

[39] R. J. Acciavatti and A. D. Maidment, ”Calculation of OTF, NPS, and DQE for oblique x-ray incidence on turbid granular phosphors,” in International Workshop on Digital Mammography, 2010, pp. 436-443.

[40] R. J. Acciavatti and A. D. Maidment, ”Optimization of phosphor-based detector design for oblique x-ray incidence in digital breast tomosynthesis,” Medical physics, vol. 38, pp. 6188-6202, 2011.adano, I. S. Kyprianou, R. J. Jennings, and J. Sempau, ”Anisotropic imaging performance in breast tomosynthesis,” Medical physics, vol. 34, pp. 4076-4091, 2007.

[41] M. Rodrigues, S. Di Maria, M. Baptista, A. Belchior, J. Afonso, J. Vena^ncio, et al., ”Influence of X-ray scatter radiation on image quality in Digital Breast Tomosynthesis (DBT),” Radiation Physics and Chemistry, vol. 140, pp. 300-304, 2017.

[42] A. Badano, M. Freed, and Y. Fang, ”Oblique incidence effects in direct x- ray detectors: A first-order approximation using a physics-based analytical model,” Medical physics, vol. 38, pp. 2095-2098, 2011.

[43] R. M. Nishikawa, I. Reiser, P. Seifi, and C. J. Vyborny, ”A new ap- proach to digital breast tomosynthesis for breast cancer screening,” in Med- ical Imaging 2007: Physics of Medical Imaging, 2007, p. 65103C.

[44] M. Das, H. C. Gifford, and S. J. Glick, ”Evaluation of a variable dose acquisition technique for microcalcification and mass detection in digital breast tomosynthesis,” Medical physics, vol. 36, pp. 1976-1984, 2009.

[45] B. Ren, T. Wu, A. Smith, C. Ruth, L. Niklason, Z. Jing, et al., ”The dependence of tomosynthesis imaging performance on the number of scan projections,” in International Workshop on Digital Mammography, 2006, pp. 517-524.

ISSN: 1992-8645 www.jatit.org E-ISSN: 1817-3195

[46] T. Wu, R. H. Moore, E. A. Rafferty, and D. B. Kopans, "A comparison of reconstruction algorithms for breast tomosynthesis," Medical physics, vol. 31, pp. 2636-2647, 2004.

[47] [49] I. Sechopoulos and C. Ghetti, "Optimization of the acquisition ge- ometry in digital tomosynthesis of the breast," Medical physics, vol. 36, pp. 1199-1207, 2009.

[48] T. Mertelmeier, J. Ludwig, B. Zhao, and W. Zhao, "Optimization of to- mosynthesis acquisition parameters: angular range and number of projections," in International Workshop on Digital Mammography, 2008, pp. 220- 227.

[49] G. M. Stevens, R. L. Birdwell, C. F. Beaulieu, D. M. Ikeda, and N. J. Pelc, "Circular tomosynthesis: potential in imaging of breast and upper cervical spine—preliminary phantom and in vitro study," Radiology, vol. 228, pp. 569-575, 2003.

[50] K. Zeng, H. Yu, S. Zhao, L. L. Fajardo, C. Ruth, Z. Jing, et al., "Digital to- mosynthesis aided by low-resolution exact computed tomography," Journal of computer assisted tomography, vol. 31, pp. 976-983, 2007.

[51] D. Xia, S. Cho, J. Bian, E. Y. Sidky, C. A. Pelizzari, and X. Pan, "To- mosynthesis with source positions distributed over a surface," in Medical Imaging 2008: Physics of Medical Imaging, 2008, p. 69132A.

[52] J. Zhang and C. Yu, "A novel solid-angle tomosynthesis (SAT) scanning scheme," Medical physics, vol. 37, pp. 4186-4192, 2010.

[53] I. Sechopoulos, S. Suryanarayanan, S. Vedantham, C. D'Orsi, and A. Karellas, "Computation of the glandular radiation dose in digital tomosyn- thesis of the breast," Medical physics, vol. 34, pp. 221-232, 2007.

[54] D. Dance, K. Young, and R. Van Engen, "Estimation of mean glandular dose for breast tomosynthesis: factors for use with the UK, European and IAEA breast dosimetry protocols," Physics in Medicine & Biology, vol. 56, p. 453, 2010.

[55] P. S. Rezentes, A. de Almeida, and G. T. Barnes, "Mammography grid performance," Radiology, vol. 210, pp. 227-232, 1999.

[56] S. S. J. Feng, C. J. D'Orsi, M. S. Newell, R. L. Seidel, B. Patel, and I. Sechopoulos, "X-ray scatter correction in breast tomosynthesis with a pre- computed scatter map library," Medical physics, vol. 41, 2014.

[57] I. Sechopoulos, S. Suryanarayanan, S. Vedantham, C. J. D'Orsi, and A. Karellas, "Scatter radiation in digital tomosynthesis of the breast," Medical physics, vol. 34, pp. 564-576, 2007.

[58] J. Lee, C. H. Lim, J.-W. Park, I.-H. Kim, M. K. Moon, and Y.-K. Lim, "The Effect of Grid Ratio and Material of Anti-scatter Grid on the Scatter- to-primary Ratio and the Signalto-noise Ratio Improvement Factor in Container Scanner X-ray Imaging," Journal of Radiation Protection and Re- search, vol. 42, pp. 197-204, 2017.

[59] J. M. Boone, K. K. Lindfors, V. N. Cooper, and J. A. Seibert,"Scatter/primary in mammography: Comprehensive results," Medical physics, vol. 27, pp. 2408-2416, 2000.

[60] G. Wu, J. G. Mainprize, J. M. Boone, and M. J. Yaffe, "Evaluation of scatter effects on image quality for breast tomosynthesis," Medical physics, vol. 36, pp. 4425-4432, 2009.

[61] O. Diaz, D. Dance, K. Young, P. Elangovan, P. Bakic, and K. Wells, "Es- timation of scattered radiation in digital breast tomosynthesis," Physics in Medicine & Biology, vol. 59, p. 4375, 2014.

[62] C. Altunbas, B. Kavanagh, T. Alexeev, and M. Miften, "Transmission characteristics of a two dimensional antiscatter grid prototype for CBCT," Medical physics, 2017.

[63] B. Liu, T. Wu, R. H. Moore, and D. B. Kopans, "Monte Carlo simulation of x-ray scatter based on patient model from digital breast tomosynthesis," in Medical Imaging 2006: Physics of Medical Imaging, 2006, p. 61421N.

[64] J. Feng, S. Si, and I. Sechopoulos, "A software-based x-ray scatter correc- tion method for breast tomosynthesis," Medical physics, vol. 38, pp. 6643- 6653, 2011.

[65] R. S. Saunders Jr, E. Samei, J. Y. Lo, and J. A. Baker, "Can compres- sion be reduced for breast tomosynthesis? Monte Carlo study on mass and microcalcification conspicuity in tomosynthesis," Radiology, vol. 251, pp. 673-682, 2009.

[66] D. Fo¨rnvik, I. Andersson, T. Svahn, P. Timberg, S. Zackrisson, and A. Tingberg, "The effect of reduced breast compression in breast tomosyn- thesis: human observer study using clinical cases," Radiation protection dosimetry, vol. 139, pp. 118-123, 2010.

[67] D. B. Kopans, Breast imaging: Lippincott Williams & Wilkins, 2007.